

1 **Supporting Information**

2

3

4 **Spectrally selective microbolometer based on planar subwavelength**

5 **thin films**

6 Qianqian Xu<sup>1,2</sup>, Ziji Zhou<sup>1,2</sup>, Chong Tan<sup>1,2</sup>, Xiaohang Pan<sup>1</sup>, Zhengji Wen<sup>1</sup>, Jinguo  
7 Zhang<sup>1, 3</sup>, Dongjie Zhou<sup>1,2</sup>, Yan Sun<sup>1</sup>, Xin Chen<sup>1</sup>, Lei Zhou<sup>4</sup>, Ning Dai<sup>1,5</sup>, Junhao  
8 Chu<sup>1,3</sup> and Jiaming Hao<sup>1,3\*</sup>

9 *<sup>1</sup> State Key Laboratory of Infrared Physics, Shanghai Institute of Technical Physics, Chinese  
10 Academy of Sciences, Shanghai 200083, China*

11 *<sup>2</sup> University of Chinese Academy of Sciences, Beijing 100049, China*

12 *<sup>3</sup> Shanghai Frontiers Science Research Base of Intelligent Optoelectronics and Perception,  
13 Institute of Optoelectronics, Fudan University, Shanghai 200433, China*

14 *<sup>4</sup> State Key Laboratory of Surface Physics and Key Laboratory of Micro and Nano Photonic  
15 Structures (Ministry of Education), and Physics Department, Fudan University, Shanghai 200433,  
16 China*

17 *<sup>5</sup> Hangzhou Institute for Advanced Study, University of Chinese Academy of Sciences, Hangzhou  
18 310024, China*

19 \*E-mail: [jmhao@fudan.edu.cn](mailto:jmhao@fudan.edu.cn)

20

21 **Supporting Information**

22

23 **Table S1:** Calculated and measured resistance of the fabricated microbolometers.

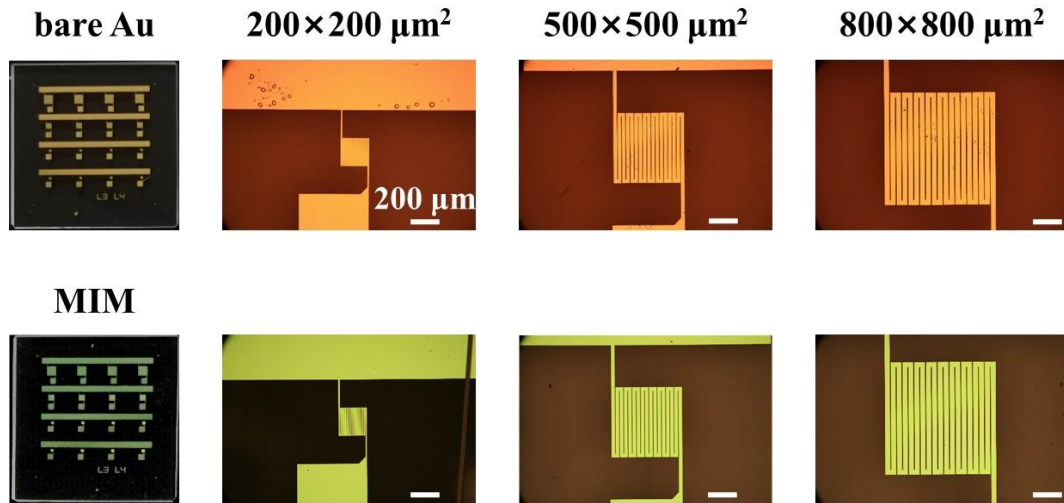
<b>Bolometers</b>	<b><math>\rho_{Au}</math> (<math>\Omega \cdot cm</math>)<sup>1</sup></b>	<b>Cal. Resistance (<math>\Omega</math>)</b>	<b>Exp. Resistance (<math>\Omega</math>)</b>
<b>bare Au-200</b>		115	115
<b>bare Au-500</b>	$3 \times 10^{-6}$	110	120
<b>bare Au-800</b>		135	146
<b>MIM-200</b>	top: $8 \times 10^{-6}$	102	104
<b>MIM-500</b>	bottom: $3 \times 10^{-6}$	98	104
<b>MIM-800</b>	(Parallel Connection)	120	134

24 **The calculated resistance ( $R$ ) is obtained by using  $R = \rho \cdot l / s$ , where  $\rho$ ,  $l$ ,  $s$  are**  
25 **the electrical resistivity, length, and cross-sectional area of the resistor,**  
26 **respectively.**

27

28

29



30

31 **Figure S1:** Photographs and microscope images of the fabricated two types

32 microbolometers with various efficient areas, scale bars are 200μm.

33

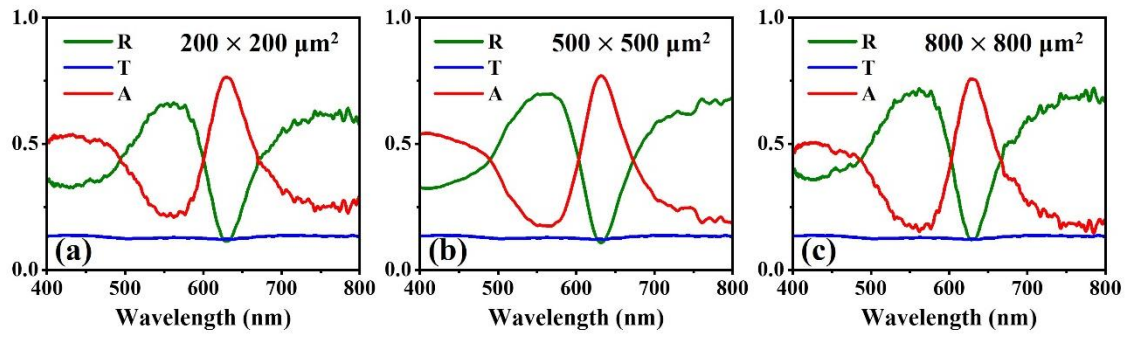
34

35

36

37

38



39

40 **Figure S2:** Experimental measured absorption spectra of the MIM microbolometers  
 41 with three area size.

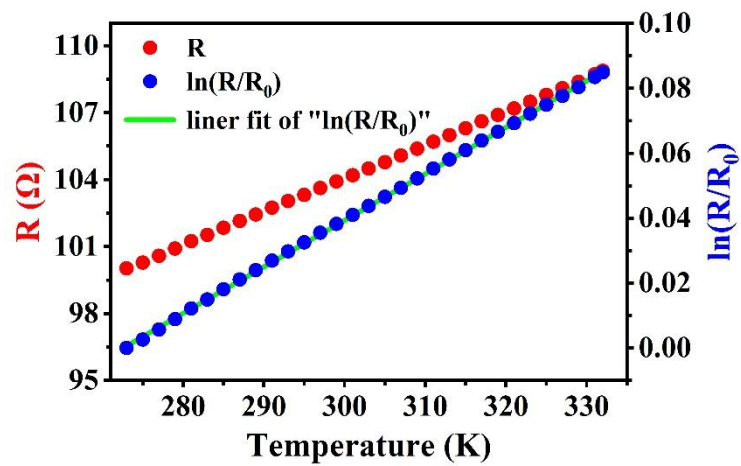
42

43

44

45

46



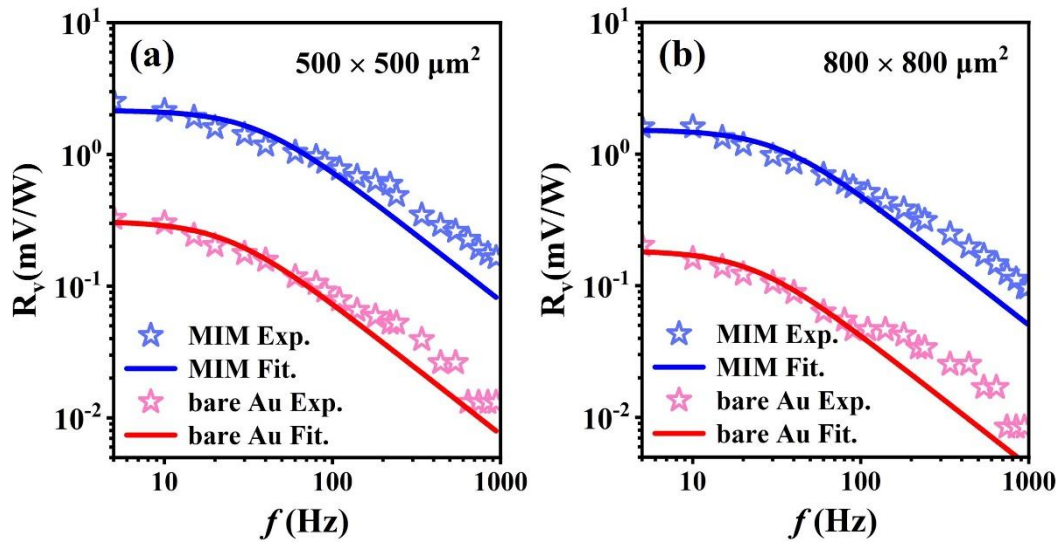
48

49 **Figure S3:** The experimentally measured the resistance change of the fabricated  
 50 microbolometer (magenta dotted line) under 0.2 mA and corresponding calculated  
 51  $\ln(R/R_0)$  (blue dotted line).  $R_0$  is the resistance of the device at temperature of 273 K,  
 52 and the fitted TCR is  $0.0014 \text{ K}^{-1}$ .

53

54

55



56

57 **Figure S4:** The experimentally measured responsivities of microbolometers with  
 58 efficient area size of  $500 \times 500 \mu\text{m}^2$ , and  $800 \times 800 \mu\text{m}^2$ , as a function of modulation  
 59 frequency.

60

61 **Note 1: Calculation of the thermal conductance**

62 The thermal conductance  $G$  can be theoretically calculated by<sup>2</sup>

$$63 \quad G = k \cdot S/h \quad (S1)$$

64 Where  $k$ ,  $S$  and  $h$  are the thermal conductivity of material, the contact area, and the  
65 heat transfer distance, respectively.

66 Firstly, 2D heat distributions were calculated based finite element methods. In the  
67 simulations, we replace the winding structure as planar thin films for both MIM and  
68 bare Au devices to simplify the calculation, the sizes and thicknesses for each film are  
69 as the real devices. The planar thin film structures serve as the heat source on a quartz  
70 substrate. The heat conductivities of gold, alumina, and quartz were taken from  
71 literature<sup>2</sup>. The thermal power density of the heat source of MIM structures is set one  
72 order of magnitude larger than that of the bare Au control samples. After getting heat  
73 distribution of each device at the response time, we then utilize the lateral heat  
74 transfer distance  $d$  and vertical heat transfer distance  $t$  obtained from the simulated  
75 results to calculate the contact area ( $S=d^2$ ) and distance ( $h=t$ ). Finally, the effective  
76 thermal conductance  $G$ , and the ratio of the absorption coefficient at 638 nm to the  
77 effective thermal conductance ( $\eta/G$ ) for each microbolometer can be calculated using  
78 Eq. (S1). The calculated results are listed in Table S2.

79

80 **Table S2:** Calculated  $G$  and  $\eta/G$  of the fabricated microbolometers.

<b>Bolometers</b>	<b><math>\tau</math> (ms)</b>	<b><math>S</math> (m<sup>2</sup>)</b>	<b><math>h</math> (m)</b>	<b><math>G</math>(W/K)</b>	<b><math>\eta/G</math></b>
<b>bare Au-200</b>	4.29	$2.03 \times 10^{-7}$	$1.50 \times 10^{-4}$	$1.86 \times 10^{-3}$	47.28
<b>bare Au-500</b>	6.60	$5.63 \times 10^{-7}$	$1.50 \times 10^{-4}$	$5.18 \times 10^{-3}$	17.02
<b>bare Au-800</b>	6.90	$1.21 \times 10^{-6}$	$2.00 \times 10^{-4}$	$8.35 \times 10^{-3}$	10.55
<b>MIM-200</b>	2.14	$1.60 \times 10^{-7}$	$1.20 \times 10^{-4}$	$1.84 \times 10^{-3}$	413.19
<b>MIM-500</b>	4.50	$5.93 \times 10^{-7}$	$1.50 \times 10^{-4}$	$5.45 \times 10^{-3}$	139.38
<b>MIM-800</b>	4.85	$1.44 \times 10^{-6}$	$1.50 \times 10^{-4}$	$1.32 \times 10^{-2}$	57.39

81

82

83 **SI references:**

84 1 G. Kästle, H. G. Boyen, A. Schröder, A. Plettl and P. Ziemann, *Phys. Rev. B*,  
85 2004, **70**, 165414.

86 2 F. P. Incropera, D. P. DeWitt, T. L. Bergman and A. S. Lavine, *Fundamentals*  
87 *of Heat and Mass Transfer*, New York: Wiley, 1996.

88